University of Glasgow

Zheng, L., Zhao, M., Dai, B., Xue, Z., Kang, Y., Liu, S., Hou, L. , Zhuang, S. and Zhang, D. (2023) Integrated system for rapid enrichment and detection of airborne polycyclic aromatic hydrocarbons. *Science of the Total Environment*, 864,161057.
(doi: 10.1016/j.scitotenv.2022.161057)

Copyright © 2022 Elsevier BV. This is the author version of the work reproduced here under a Creative Commons Attribution-NonCommercial-NoDerivs 4.0 licence: https://creativecommons.org/licenses/by-nc-nd/4.0/ .

There may be differences between this version and the published version. You are advised to consult the publisher's version if you wish to cite from it: https://doi.org/10.1016/j.scitotenv.2022.161057

https://eprints.gla.ac.uk/288004/

Deposited on: 16 December 2022

Enlighten – Research publications by members of the University of Glasgow
http://eprints.gla.ac.uk

Manuscript (double-spaced and continuously LINE and PAGE numbered)-for final publication

Click here to view linked References

Integrated System for Rapid Enrichment and Detection of Airborne Polycyclic Aromatic Hydrocarbons

Authors: Lulu Zheng [a,1], Mantong Zhao [b,1], Bo Dai [a,1], Zhiwei Xue [a], Yi Kang [a], Sixiu Liu [c*], Lianping Hou [d], Songlin Zhuang [a], Dawei Zhang [a,e*]

[a] Engineering Research Center of Optical Instrument and System, Ministry of Education, Shanghai Key Lab of Modern Optical System, Shanghai Environmental Biosafety Instruments and Equipment Engineering Technology Research Center, University of Shanghai for Science and Technology, 516 Jungong Road, Shanghai 200093, China

[b] College of Physics and Electronic Engneering, Heze University, 2269 Daxue Road, Shandong 274015, China

[c] Shanghai Key laboratory of Atmospheric Particle Pollution Prevention (LAP3), Department of Environmental Science & Engineering, Fudan University, 220 Handan Road, Shanghai 200433, P.R. China

[d] James Watt School of Engineering, University of Glasgow, Glasgow G12 8QQ, U.K.

[e] Department of Hepatic Surgery VI, Eastern Hepatobiliary Surgery Hospital, Second Military Medical University. Shanghai, China

[1] Lulu Zheng, Mantong Zhao and Bo Dai contributed equally to this work.

*Corresponding authors: E-mail: liusixiu@163.com; dwzhang@usst.edu.cn

ABSTRACT

Polycyclic aromatic hydrocarbons (PAHs) are extremely toxic environmental pollutants, which are harmful to the human body. Direct collection and analysis of airborne PAHs is essential for air quality monitoring. Herein, we demonstrated an integrated system for airborne PAHs enrichment and detection. The enrichment cube was composed of channels with threaded structures and curved channels, which had high capture efficiency. Then PAHs-carried particles could be crushed into the detection chip for testing. The whole process took about 25 min (5 min for PAHs enrichment and 20 min for PAHs test). The limit of detection was 3.3 ng/m^3, which could meet the needs of daily analysis. It had the advantages of low cost, low reagent consumption, simple operation, semi-automatic operation, high sensitivity, high speed and high throughput compared with conventional techniques, showing the potential for becoming an air pollution monitoring platform.

KEYWORDS:

Integrated system; Semi-automatic operation; Enrichment cube; Immunoassay chip; PAHs

1. Introduction

Air pollution has emerged as a serious problem in many countries worldwide, especially in developing countries(Hamidi et al., 2020; Madhuri et al., 2021). PM2.5 makes the greatest contribution to air pollution(Zhang et al., 2018). Among the organic components of PM2.5, polycyclic aromatic hydrocarbons (PAHs) are the most obtrusive(Zhang et al., 2021). PAHs are a group of organic compounds primarily produced by the incomplete combustion of fossil fuels(Sun et al., 2020; Verma et al., 2018). As carcinogenic, teratogenic, and genotoxic compounds, PAHs can cause great damage to human health. Moreover, longtime exposure to PAHs leads to the increased

prevalence of various diseases (such as lung diseases, cardiovascular diseases, and skin diseases) and genetic mutation(Liu et al., 2017; Shippi et al., 2014). Therefore, considering the wide range of potential harm caused by PAHs, it was of great necessity to monitor the daily concentrations of PAHs.

The analysis step of airborne PAHs consisted of PAH sampling, extraction, and final detection, each step conducted separately(Pandey et al., 2011). To rapidly detect PAHs, efficient sampling of fine particles in the airborne is an essential precondition. Various sampling methods have been reported, such as Andersen samplers, slit samplers, centrifugal sampler, AGI-like samplers(Pandey et al., 2011), and filters. According to an investigation, sampling by solid impactors is followed by sample extraction and suspension, while sampling by liquid impactors can avoid sample extraction and resuspension. Therefore, it is preferable to sample directly into liquid media; however, the time of sampling by liquid impactors costs about 24 h(Li et al., 2017). Regarding the final detection of PAHs, the traditional detection methods include high performance liquid chromatography with fluorescence detection (HPLC-FLD)(Walgraeve et al., 2015), gas chromatography coupled with mass spectrometer (GC/MS)(Ekner et al., 2021), liquid chromatograph-mass spectrometer (LC-MS)(Merlo et al., 2020), and surface-enhanced Raman spectroscopy(SERS)(Gu et al., 2016). Unfortunately, these methods are limited in point-of-care test (POCT) due to their complicated operating steps, expensive equipment, and long analysis time. However, transferring suspended particles to analytical systems remains the bottleneck of POCT. Therefore, it is urgent to develop a system that integrates PAHs sampling, extraction, and detection, thereby achieving the simple, rapid, and low-cost detection of air PAHs.

3D printing is a type of rapid prototyping technology with the advantages of low cost, fast speed, and convenient production(Macdonald et al., 2014). Microfluidics, a novel

technique, could control and operate micro-scale fluid with great precision(Whitesides., 2006; Eric et al., 2014; Zhu et al., 2017). Moreover, it could flexibly combine multiple function units (including sample preparation, reaction, separation, and test), showing great potential in integration and miniaturization(Wang et al., 2016). Additionally, compared with traditional analytical techniques, microfluidics also has the advantages of a simple procedure, fast reaction rate, and high sensitivity (H. Wang et al., 2021; Z. Wang et al., 2021).

Herein, we combined enrichment and detection to develop an integrated semi-automatic system, which composed of an enrichment cube and detection chip for airborne PAHs-carried particle. The design of multi-channel with threaded structures and curved channels in the enrichment cube for PAHs sampling contributes to realizing high flow and high efficiency. The detection chip had immune structures and valves to enrich and identify PAHs. The detection capability of the detection chip was validated using flow cytometric analysis. For verifying the feasibility of the integrated system, samples collected from the air were tested using the system. Compared with previously reported methods of PAHs sampling, extraction, and detection, this method allows PAHs to flow from the enrichment cube to the detection chip directly without extraction steps. The system also provided advantages, such as semi-automation, high sensitivity, high throughput, and high analysis speed, showing excellent capability for monitoring PAHs in the air and exhibiting great potential to realize the POCT with a portable fluorescence detector.

2. Methods and materials

2.1 Materials and Reagents

PAHs was supplied by the Resources Platform of the National Standard Material. Microspheres were supplied by Bangs Laboratories (Indiana, USA). The 2.5 μm

fluorescent beads were obtained from Beisile Laboratories (Tianjin, China). Anti-PAHs mouse monoclonal antibody was obtained from Santa Cruz Biotechnology (USA). Fluorescein isothiocyanate (FITC)-conjugated anti-mouse secondary antibody was obtained from Abcam Inc. (Cambridge, MA, USA). Photoresist (SU-8 2025) was obtained from Microchem (USA). Polydimethylsiloxane (PDMS) was supplied by Dow Corning Corporation (Midland, MI, USA). Tween20, phosphate-buffered saline (PBS), and other reagents were purchased from Sigma-Aldrich (St. Louis, MO, USA).

2.2. Fabrication of system

The presented system mainly consisted of two parts, airborne PAHs-carried particle enrichment cube and detection chip. The airborne PAHs-carried particle enrichment cube was designed by INVENTOR (USA), made of photosensitive resin, and fabricated by nanoArch P150 3D printing system (China) (Nagarajan et al., 2018). The detection chip consisted of two layers (a fluidic layer and a control layer) designed by AutoCAD and fabricated concerning the soft lithography process(Qin et al., 2010; Lee et al., 2005). The silicon molds of the two layers were made from SU-8 2050 photoresist. A film of photoresist was covered on a silicon wafer and then baked again. After exposure to UV light by lithography machine (SUSS, Germany) and baked, the microstructures were developed on the mold. After development, the silicon mold was achieved. According to the same procedures, the silicon mold of valve layer was completed. Afterwards, microstructures of the two layers were casted by PDMS. To prepare the fluid layer, PDMS was poured onto the mold of fluidic layer. Then degassed, and baked for an hour at 80 °C. After that, the PDMS sheet of fluid layer was detached from the silicon mold, and holes for liquid to flow was punched in the PDMS sheet. A film of PDMS was covered on the silicon mold of valve layer by spin coating for 50s at 1400 rpm and baked. Next, the two PDMS plates of fluidic and valve layer were carefully assembled.

The PDMS sheet was punched for the flow of the gas. Finally, the assembled plates were bonded to a glass sheet covered with a film of PDMS.

Following the completion of the enrichment cube and detection chip, the integrated system could be established. Specifically, the system consisted of an enrichment cube, detection chip, syringe pump, vacuum pump, and wash buffer. In the platform, the enrichment system and the detection system cooperated conveniently.

2.3. Airborne PAHs-carried particle collection by the enrichment cube

To verify the capture capacity of the enrichment cube, we stimulated the generation of airborne PAHs-carried particles and establish the enrichment efficiency detection system. In this work, 2.5 μm fluorescent beads with a similar form to that of the particulate matters were selected to simulate particulate matters. The prepared fluorescent beads suspension was used to spray fluorescent beads-aerosol droplets into a cube under the action of a mini-generator (BSW-2A, China). During the generation of fluorescent beads-aerosol, the mini-generator added with fluorescent beads suspension conducted the atomization process for 50 s at the beginning of the generation and then sprayed for 10 s every 30 s. The controller could control the generation process. When the collection process was conducted, the fluorescent beads-aerosol was inhaled into the cube using a vacuum pump, and the uncollected beads were collected using the waster collector.

After enrichment, the collected fluorescent beads in the cube were washed using PBS. After that, for evaluating the enrichment efficiency of the cube, the fluorescent beads in the enrichment cube and waster collector were counted using a flow cytometer (BD FACMelody, USA).

2.4. Analysis by the integrated airborne PAHs-carried particle enrichment and detection system

After airborne PAHs-carried particle enrichment, the detection was conducted by the detection chip. Following the injection into the reaction column, the microspheres could be intercepted in the channel with the action of the sieve valves. Next, the collected airborne PAHs-carried particles in the washing buffer were injected into the detection chip, with the inlet flow rate controlled at 5 μL min^{-1}. After that, the detection chip was placed at room temperature away from light for a 5-min reaction, followed by reaction column washing using PBS-Tween-20 (PBST) solution. Thereafter, anti-PAHs monoclonal antibody was injected into the reaction channel, and the chip was incubated (37°C, 10 min) away from light. After washing the microspheres in the reaction column using PBST solution, FITC-labeled secondary antibody solution was injected into the reaction channel, and the chip underwent an incubation (37°C, 5 min) avoiding light. Afterward, the reaction column was rinsed using PBST solution. Finally, the fluorescence images of microspheres were obtained using a fluorescence microscope (Olympus BX53, Japan). The mean fluorescence intensity values were analyzed using the Image J software.

For the quantitative detection of PAHs, different concentrations (0.033, 0.013, 0.0067, 6.67×10^{-4}, 1.3×10^{-4}, 6.7×10^{-5}, and 2.2×10^{-5} g/L) of PAHs were used to develop a standard curve by the detection chip. The fluorescence intensity of each concentration was obtained from three independent measurements. Finally, according to the standard curve, the concentration of airborne PAHs in the enrichment cube could be calculated.

2.5. Flow cytometric analysis

To validate the detection capability of the detection chip, we detected immune reactions on microspheres by flow cytometric in this study(Hui et al., 2014). Different concentrations of PAHs were prepared (6.67×10^{-7}, 6.67×10^{-6}, 2.22×10^{-5}, 6.67×10^{-5}, 1.33×10^{-3}, 6.67×10^{-3}, 3.33×10^{-2}, and 6.67×10^{-2} g/L), which were then used for 1-h

incubation with aliquots (2 μL, 10 mg/mL) of microspheres at room temperature in the dark. Next, the microspheres were separated from the suspension through centrifugation (1500 rpm, 30 s), followed by 3 washes with PBST. After that, the anti-PAHs monoclonal antibody was added for incubation (37°C, 1 h) without light. Next, after 3 washes by PBST, microspheres were incubated (37°C, 30 min) with FITC-labeled secondary antibody solutions, followed by PBST washing three times. Finally, the fluorescence intensity of microspheres was detected using a flow cytometer (BD FACMelody, USA) that could emit light of 488 nm. Three independent measurements were conducted. The calibration curve was established.

2.6. Preparation of samples in the natural environment

In order to confirm the reliability of the integrated enrichment and detection system, we tested samples collected from the air. Airborne particulate PAHs were collected using a glass fiber filter (GFF) with a sampling time of 24 h and then cut into 1 cm^2 pieces. After that, sonicated in 3 ml acetonitrile for half an hour at 20℃ loaded with sample bottle (15 mL, ThermoFisher). After that, particulate PAHs were separated from acetonitrile via filters and suspended in PBS. Finally, PAHs collected from air were prepared. Then, PAHs were collected by the enrichment cube. One part of the enriched PAHs was used for ELISA and the other part was tested by the detection chip.

2.7. ELISA

To verify the accuracy of the detection chip, we detected the particulate PAHs using ELISA. Specifically, the anti-PAHs mouse monoclonal antibody was incubated (4°C, overnight) in 96-well black ELISA plates. The plate was washed with PBST and then added with 400 μL BSA for incubation (room temperature, 1 h). After that, samples obtained from the air collected by the enrichment cube were added to the wells and reacted (37°C, 1 h) with the antibody away from light. After 3 washes, the fluorescence

intensities of the PAHs were detected by Microplate Reader (Thermo Scientific A51119600C, USA) based on the autofluorescence of PAHs.

3. RESULTS AND DISCUSSION

3.1. Design and validation of PAHs enrichment cube

The enrichment cube was designed by INVENTOR, and fabricated by 3D printing, as shown in Figure 1A and Figure 1B. The enrichment cube was composed of 16 channels with threaded structures, and each channel had 12 paths. These 12 paths were connected by curved channels (Figure 1C). Based on aerodynamic principles, the suspended airborne PAHs-carried particle could be sampled on the inner surface of the cube. Numerical simulation of airflow dynamics inside the curved channel was performed using CMOSOL. As shown in Figure 1D, when passing through the curved channel, aerosols moved radially outward due to centrifugal force. The threaded structures were introduced into the inner surface of the enrichment cube for collecting the particulate matters, which could transform the laminar air flow into a chaotic flow when aerosols were introduced into the channel. Compared to channels without structure, channels with threaded structures had a much larger surface area (increased 854 mm^2), which would increase the contact area between particulate matters and the inner surface of the cube. Compared with the planar staggered herringbone mixer (SHM) structure in the microfluidic channels(Jing et al., 2013), this structure had a surface area increased by nearly nine times. In the process of enrichment, 16 channels could enrich particulate matters in parallel through the action of the vacuum pump. As a result, more airborne PAHs-carried particles could be attached to the surface of the cube, thereby improving the efficiency and reducing the time. The flow of the cube could be up to 20 L/min. After the collection of the particulate matters, the channel for particulate matters collection was washed using PBS buffer. The airborne PAHs-carried particle attached

to the surface of the particulate matters in the eluent could be immediately tested in the downstream microfluidic detection chip, thus achieving the integration of sampling and detection.

In this study, the feasibility of the enrichment cube was verified, and the enrichment detection system was established (Figure 2A). The cube was detected by ChemiDoc (BIO-RAD, USA) for evaluating the capture of the fluorescent beads. Figure 2 showed the distribution of fluorescent beads in the enrichment cube within 1-min enrichment time. In this study, fluorescent beads that could emit green fluorescence when excited by blue light were used. The results indicated that fluorescent beads adhered to the internal surface of the cube; the cube could achieve the enrichment of particulate matters. Moreover, the fluorescence intensity of fluorescent beads adhered to the internal surface of the cube was detected. As revealed in Figure 2B, the brightness of fluorescent beads was diminished and the fluorescence intensity was gradually decreased along the channel from inlet to outlet. Additionally, fluorescence was not detected from the 11^{th} channel.

To explore the enrichment efficiency of the cube at different times, we studied 5 different experimental times. As shown in Table 1, the enrichment efficiency exceeded 97% in the first 15 min, reaching 100% at the highest (Jing, et al., 2013), which was higher than that of traditional methods (Pandey et al., 2011). The results suggested that the cube exhibited obvious effects on capturing particulate matters from the aerosol. A previous report has pointed out that the sampling time was more than 24 h by the traditional sampling method(Pandey et al., 2011). Therefore, compared with traditional sampling methods, sampling by the cube provided less time and higher enrichment efficiency.

3.2. Design and validation of PAHs detection chip

The detection chip was used for PAH detection. The detection chip (5 × 5 cm^2) consisted of two layers (fluidic layer and control layer) (Figure 3A). The detection chip had 8 test units, and each unit consisted of valves and reaction columns (200 μm wide × 30 μm high). Multiple samples were tested through the control of the valves and detected in reaction columns. Wash buffer and antibody inlet were shared by 8 detection units, and each channel had its respective sample and microspheres inlet. The valves in the control layer consisted of two valves (regular valves and sieve valves) (Figure 3B).

Regular valves made the channel a closed space, while sieve valves could intercept microspheres (20 μm in diameter) and didn't work on the liquid reagent. With the collaboration of regular valves and sieve valves, sample tests could be performed sequentially or simultaneously according to practical applications. Compared with traditional methods, the microspheres were closely arranged in the reaction column, which provided a larger surface area to bind PAHs. Considering the small dimensions of the channel, the consumption of samples and reagents was reduced, and the reaction rate was markedly increased.

Microspheres with the size of about 20 μm were used in this study to adsorb and collect particle matters carrying PAHs. The schematic diagram of PAH detection on microspheres was illustrated in Figure 4A. There were two reasons for PAHs capture by the microspheres. Firstly, the microspheres are polystyrene microplastic that can adsorb PAHs(Avio et al., 2015; Liu et al., 2016). Secondly, the microspheres were modified by carboxyl (-COOH), which can adsorb a small amount of PAHs to expand the curled edges, thereby generating new potential adsorption sites and improving the adsorption abilities of PAHs(Wang et al., 2014). Considering that the plastics-based microsphere with the carboxyl group could catch PAHs through physisorption, and specific recognition by PAHs antibody, the high-efficiency PAHs detection based on

microfluidic chips could be realized.

The immunoassay protocol by the microfluidic detection chip was illustrated in Figure 4B. PAHs concentration was adjusted to 0.033, 0.013, 0.0067, 6.67×10^{-4}, 1.3×10^{-4}, 6.7×10^{-5}, and 2.2×10^{-5} g/L and the fluorescence images of PAHs in the reaction column were shown in Figure 5(a-g). Figure 5A-h was blank control, which was the image of microspheres in the chip under 488 nm excitation, indicated that fluorescence detection could be performed with no interruption of background. The calibration curve shown in Figure 5B indicated that the fluorescence intensity was increased with the increase of PAHs concentration. The R^2 was 0.945, which was suitable for quantitative analysis.

3.3. PAHs detection by flow cytometry

For verifying the microfluidic immunoassay chip, the fluorescence intensity of various concentrations of PAHs coated on microspheres was tested using flow cytometry. And the calibration curve showed the fluorescence intensity was increased with the PAHs concentration, and R^2 was 0.946 (Figure 6). These results indicated that microspheres based on immunoassay can be used to detect PAHs.

3.4. Integrated semi-automated PAHs enrichment and detection system

After the fabrication and test of the enrichment and detection system, the integrated system was established (Figure 7). When the particle matters sampling was completed, wash buffer was injected into the enrichment cube for channel washing, and particle matters carrying PAHs were flushed into the microfluidic immunoassay chip to detect PAHs with the effect of the injection pump. The microfluidic immunoassay chip had 8 units, and each unit could connect an enrichment cube.

We designed the micro-valve control system which consisted of electromagnetic solenoid valves, and the integrated enrichment and detection system could be set to

manual or semi-automatic with the effect of the micro-valve control system according to the program settings. Therefore, the integrated system could realize PAHs semi-automated high-throughput quantitative detection.

3.5. Validation of the enrichment and detection system

When the sampling time was 5 min, the calculated limit of detection (LOD) was 3.3 ng/m^3 via the flow rate of the vacuum pump and the experimental results of the enrichment and detection system. The actual concentration of PAHs in the air monitored for 20 days in a certain area was obtained by relevant departments (Table 2). It was found that concentrations of PAHs in the air were above 3.3 ng/m^3. Therefore, the LOD of the system could meet the practical detection needs in the actual environment.

3.6. Detection of samples in the natural environment

For verifying the feasibility of the proposed enrichment and detection system, samples in air collected by enrichment cube were tested by the detection system and ELISA. The results of the system were consistent with those of ELISA, and the R^2 was 0.980 (Figure 8). These results indicated that the proposed system could realize the quantitative analysis of PAHs in the air and truly meet the needs of integration of sampling and detection.

4. Conclusion

In the present study, an integrated PAHs-carried particles enrichment and detection system was developed to directly analyze airborne PAHs. A 3D printing enrichment cube chip was fabricated, which had increased surface area by nearly nine times than the SHM structure chip. Furthermore, when passing through the curved channel, aerosols move radially outward due to centrifugal force. Therefore, high efficacy enrichment could be achieved using the enrichment cube chip. After sampling airborne PAHs by the enrichment cube, the PAHs eluent could be directly used in the detection

system, thereby actually realizing the integration of enrichment and detection. The whole process took about 25 min (5 min for PAHs enrichment and 20 min for airborne PAHs test in the system), which was much less than the conventional method that took about 28 h (collection by particulates collector and detection by ELISA). Moreover, the detection limit of the system was 3.3 ng/m^3, which could meet the requirements for routine analysis. Additionally, fluorescence intensity could be read by a hand-held fluorescence microscope developed by our lab(Dai et al., 2019), thus achieving POCT. With the advantages of short time, high precision, simple operation, less reagent consumption, high throughput, and semi-automatic operation, this system proposed in this study realized the analysis of PAHs from the air. Therefore, this method could effectively monitor the air quality and provided a basis for decision-making in the control and treatment of air pollution problems.

Acknowledgements

This research was supported by Ministry of Science and Technology of China (2021YFE0111300), Shanghai Science and Technology Commission (22140900900), Doctoral Scientific Research Foundation of Heze University(XY21BS34).

Notes

The authors declare that they have no known competing financial interests or personal relationships that could have appeared to influence the work reported in this paper.

References

Avio, C.G., Gorbi, S., Milan, M., et al. 2015. Pollutants bioavailability and toxicological risk from microplastics to marine mussels. Environmental Pollution. 198, 211-222. https://doi.org/10.1016/j.envpol.2014.12.021.

Dai, B., Jiao, Z., Bachman, H., et al. 2019. Colour compound lenses for a portable fluorescence

microscope. Light: Science & Applications. 8, 1-13. https://doi.org/10.1038/s41377-019-0187-1.

Eduati, F., Utharala, R., Madhavan, D., et al. 2018. A microfluidics platform for combinatorial drug screening on cancer biopsies. Nature communications. 9(1), 1-13. https://doi.org/10.1038/s41467-018-04919-w.

Ekner, H., Dreij, K., Sadiktsis, I., 2021. Determination of polycyclic aromatic hydrocarbons in commercial olive oils by HPLC/GC/MS – Occurrence. composition and sources. Food Control. 132, 108528. https://doi.org/10.1016/j.foodcont.2021.108528.

Eric, K.S., Anna, L.F., David, J.B., 2014. The present and future role of microfluidics in biomedical research. Nature. 507, 181-189. https://doi.org/10.1038/nature13118.

Gu, H.X., Hu, K., Li, D.W., et al. 2016. SERS detection of polycyclic aromatic hydrocarbons using a bare gold nanoparticles coupled film system. Analyst. 141(14), 4359-4365. https://doi.org/10.1039/c6an00319b.

Hamidi, A., Ramavandi, B., 2020. Evaluation and scientometric analysis of researches on air pollution in developing countries from 1952 to 2018. Air Quality Atmosphere & Health. 13(12), 797-806. https://doi.org/10.1007/s11869-020-00836-4.

Hui, Y.Y., Su, L.J., Chen, O.Y., et al. 2014. Wide-field imaging and flow cytometric analysis of cancer cells in blood by fluorescent nanodiamond labeling and time gating. Scientific Reports. 4, 1-7. https://doi.org/10.1038/srep05574.

Jing, W., Zhao, W., Liu, S., et al. 2013. Microfluidic device for efficient airborne bacteria capture and enrichment. Analytical chemistry. 85(10), 5255-5262. https://doi.org/10.1021/ac400590c.

Lee, C. C., Sui, G., Elizarov, A.,et al. , 2005. Multistep Synthesis of a Radiolabeled Imaging Probe Using Integrated Microfluidics. Science, 310(5755), 1793–1796. https://doi.org/ 10.1126/science.11

18919.

Li, Y., Xian, Q., Li, L., 2017. Development of a short path thermal desorption-gas chromatography/mass spectrometry method for the determination of polycyclic aromatic hydrocarbons in indoor air. Journal of Chromatography A. 1497, 127-134. https://doi.org/10.1016/j.chroma.2017.03.050.

Liu, D., Lin, T., Syed, J.H., et al. 2017. Concentration, source identification, and exposure risk assessment of PM2.5-bound parent PAHs and nitro-PAHs in atmosphere from typical Chinese cities. Scientific Reports. 7, 1-12. https://doi.org/10.1038/s41598-017-10623-4.

Liu, L., Fokkink, R., Koelmans, A.A., 2016. Sorption of polycyclic aromatic hydrocarbons to polystyrene nanoplastic. Environmental Toxicology & Chemistry. 35(7), 1650-1655. https://doi.org/10.1002/etc.3311.

Macdonald, E., Salas, R., Espalin, D., et al. 2014. 3D Printing for the Rapid Prototyping of Structural Electronics. IEEE Access. 2(2), 234-242. https://doi.org/10.1109/ACCESS.2014.2311810.

Madhuri, V., Shamsh, P., Judith C. C. et al. 2021. Assessing the magnitude of PM2.5 polycyclic aromatic hydrocarbon emissions from residential solid fuel combustion and associated health hazards in South Asia, Atmospheric Pollution Research, 12 (8): 101142, https://doi.org/10.1016/j.apr.2021.101142.

Merlo, T.C., Molognoni, L., Hoff, R.B., et al. 2020. Alternative pressurized liquid extraction using a hard cap espresso machine for determination of polycyclic aromatic hydrocarbons in smoked bacon. Food Control. 120, 107565. https://doi.org/10.1016/j.foodcont.2020.107565.

Nagarajan, B., Eufracio Aguilera, A. F., Wiechmann, M., et al. 2018. Characterization of magnetic particle alignment in photosensitive polymer resin: A preliminary study for additive manufacturing processes. Additive Manufacturing. 22, 528–536.

https://doi.org/10.1016/j.addma.2018.05.046.

Pandey, S.K., Kim, K.H., Brown, R., 2011. A review of techniques for the determination of polycyclic aromatic hydrocarbons in air. Trac Trends in Analytical Chemistry. 30(11), 1716-1739. https://doi.org/10.1016/j.trac.2011.06.017.

Qin, D., Xia, Y., Whitesides, G.M., 2010. Soft lithography for micro- and nanoscale patterning. Nature Protocols. 5, 491-502. https://doi.org/10.1038/nprot.2009.234.

Shippi D., Shamsh P., Rajan C., et al. 2014. Uncharted sources of particle bound polycyclic aromatic hydrocarbons from South Asia: Religious/ritual burning practices, Atmospheric Pollution Research, 5 (2): 283-291. https://doi.org/10.5094/APR.2014.034.

Sun, B., Shi, Y., Li, Y., et al. 2020. Short-term PM_(2.5) exposure induces sustained pulmonary fibrosis development during post-exposure period in rats. Journal of Hazardous Materials. 385(5), 121566. https://doi.org/10.1016/j.jhazmat.2019.121566.

Verma M. A., Pervez S. H., Deb M. K., et al.2018. Domestic use of cooking fuel in India: a review on emission characteristics and associated health concerns. Asian Journal of Chemistry. 30(2), 235-45. https://doi.org/10.14233/ajchem.2018.21006.

Walgraeve, C., Chantara, S., Sopajaree, K., et al. 2015. Quantification of PAHs and oxy-PAHs on airborne particulate matter in Chiang Mai, Thailand, using gas chromatography high resolution mass spectrometry. Atmospheric Environment. 107, 262-272. https://doi.org/10.1016/j.atmosenv.2015.02.051.

Wang, D., Wang, J., Yang, Y., et al. 2021. Formation mechanism of heavy haze-fog associated with the interactions between different scales of atmospheric processes in China. Atmospheric Pollution Research. 12(8), 101085. https://doi.org/10.1016/j.apr.2021.101085.

414 Wang, H., Zhang, Y. L., Han, D. D., Wang, W., & Sun, H. B. 2021. Laser fabrication of modular
415 superhydrophobic chips for reconfigurable assembly and self-propelled droplet manipulation.
416 *PhotoniX*, *2*(1). https://doi.org/10.1186/s43074-021-00033-1.
417 Wang, J., Brisk, P., William, H., 2016. Random design of microfluidics. Lab on a chip. 16(21), 4212-
418 4219. https://doi.org/10.1039/c6lc00758a.
419 Wang, J., Chen, Z., Chen, B., 2014. Adsorption of polycyclic aromatic hydrocarbons by graphene and
420 graphene oxide nanosheets. Environmental Science & Technology. 48(9), 4817-4825.
421 https://doi.org/10.1021/es405227u.
422 Wang, Z., Liu, Y., Gong, C., Yuan, Z., Shen, L., Chang, P., Liu, K., Xu, T., Jiang, J., Chen, Y. C., & Liu,
423 T. 2021. Liquid crystal-amplified optofluidic biosensor for ultra-highly sensitive and stable
424 protein assay. *PhotoniX*, *2*(1). https://doi.org/10.1186/s43074-021-00041-1.
425 Whitesides, G.M., 2006. The origins and the future of microfluidics. Nature. 442(7101), 368-373.
426 https://doi.org/10.1038/nature05058.
427 Zhang, Y., Lang, J., Cheng, S., et al. 2018. Chemical composition and sources of PM_1 and $PM_{2.5}$ in
428 Beijing in autumn. Science of The Total Environment. 630, 72-82. DOI:
429 https://doi.org/10.1016/j.scitotenv.2018.02.151.
430 Zhang, Y., Song, Y., Chen, Y.J., et al. 2021. Discovery of emerging sulfur-containing PAHs in PM2.5:
431 contamination profiles and potential health risks. Journal of Hazardous Materials. 416, 1-10.
432 https://doi.org/10.1016/j.jhazmat.2021.125795.
433 Zhu, P., Wang, L., 2017. Passive and active droplet generation with microfluidics: a review. Lab on a
434 chip. 17, 34-75. https://doi.org/10.1039/C6LC01018K.
435

Figure Captions

Figure 1： PAHs enrichment cube and principle scheme of aerosol sampling in the cube. A) The design diagram of the airborne PAHs-carried particle enrichment cube and partial enlarged drawing. B) The image of real enrichment cube. C) The principle scheme of aerosol sampling in the cube. D) Numerical simulations of airflow dynamics inside the curved channel.

Figure 2： The validation of PAHs enrichment cube. A) The enrichment detection system. B) The distribution of fluorescent beads in the enrichment cube.

Figure 3： The detection chip of PAHs. A) The design of the PAH detection chip. B) Enlarged image of the test unit in the detection chip. C) The image of the PAH detection chip.

Figure 4： The principle of immunoassay in the microfluidic chip. A) The schematic diagram of immunoassay on microspheres. B) The sequence diagram of PAHs detection in the microfluidic chip.

Figure 5： Quantitative detection of PAHs by the microfluidic chip. A) The fluorescence images of reaction columns for different concentrations of PAHs. B) The calibration curve for detecting the concentration of PAHs.

Figure 6： The results of the PAHs detection by flow cytometry. A) The mean fluorescence intensity of different concentrations of PAHs by flow cytometry. B) The calibration curve between different concentrations of PAHs and mean fluorescence intensity.

Figure 7： The integrated PAHs enrichment and detection system.

Figure 8： The comparison results of the integration system and ELISA.

Table 1(Editable version)
Click here to access/download;Table (Editable version);Table1.docx

Table 1 The enrichment efficiency of the cube

Time (min)	Enrichment efficiency
0	0
2.3	100.00%
4	100.00%
5	99.10%
10	98.80%
15	97.20%
25	94.10%

Table 2(Editable version)
Click here to access/download;Table (Editable version);Table2.docx

Table 2 Practical concentrations of PAHs in the air for 20 days

Samples	PAHs concentrations（ng/m^3）	Samples	PAHs concentrations（ng/m^3）
1	10.094	11	11.5224
2	8.2689	12	15.241
3	9.2482	13	42.8153
4	12.2614	14	62.5591
5	9.1032	15	52.2318
6	7.6232	16	48.0771
7	41.0429	17	28.6272
8	13.9128	18	19.148
9	10.5663	19	15.6816
10	14.684	20	6.934

Figure 1

Click here to access/download;Figure;Figure 1.jpg

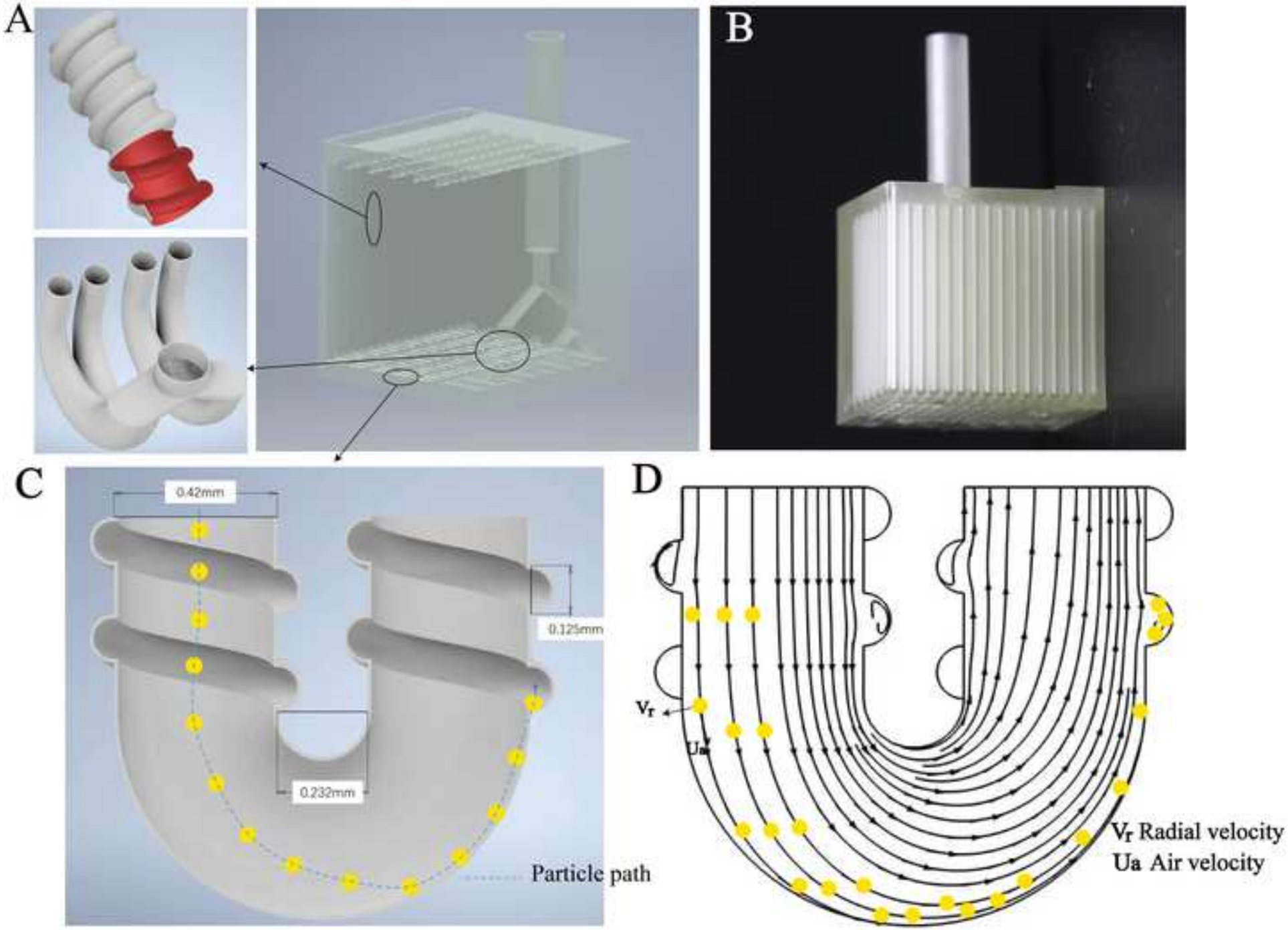

Figure 2

Click here to access/download;Figure;Figure 2.jpg

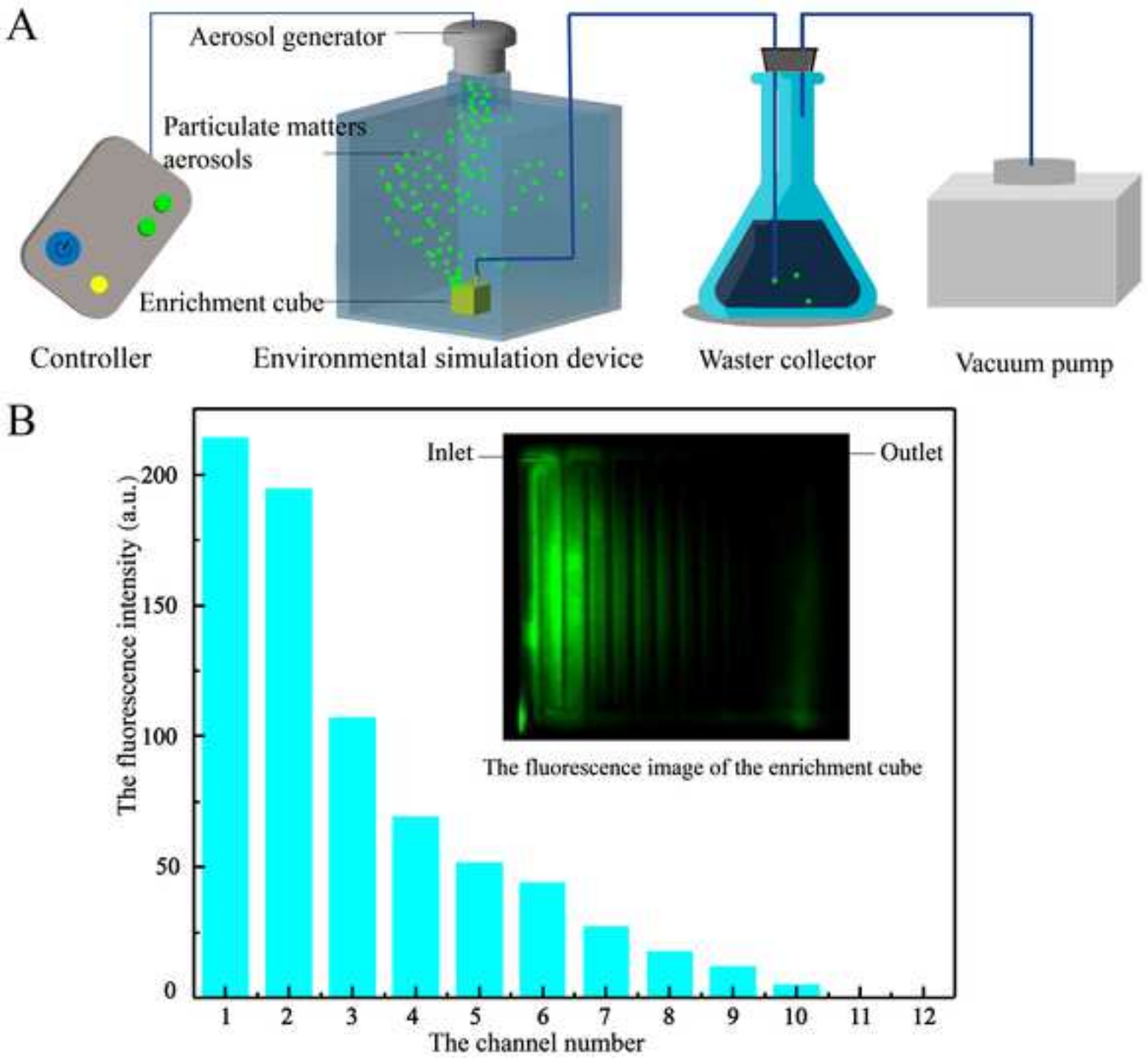

Figure 3

Click here to access/download;Figure;Figure 3.jpg

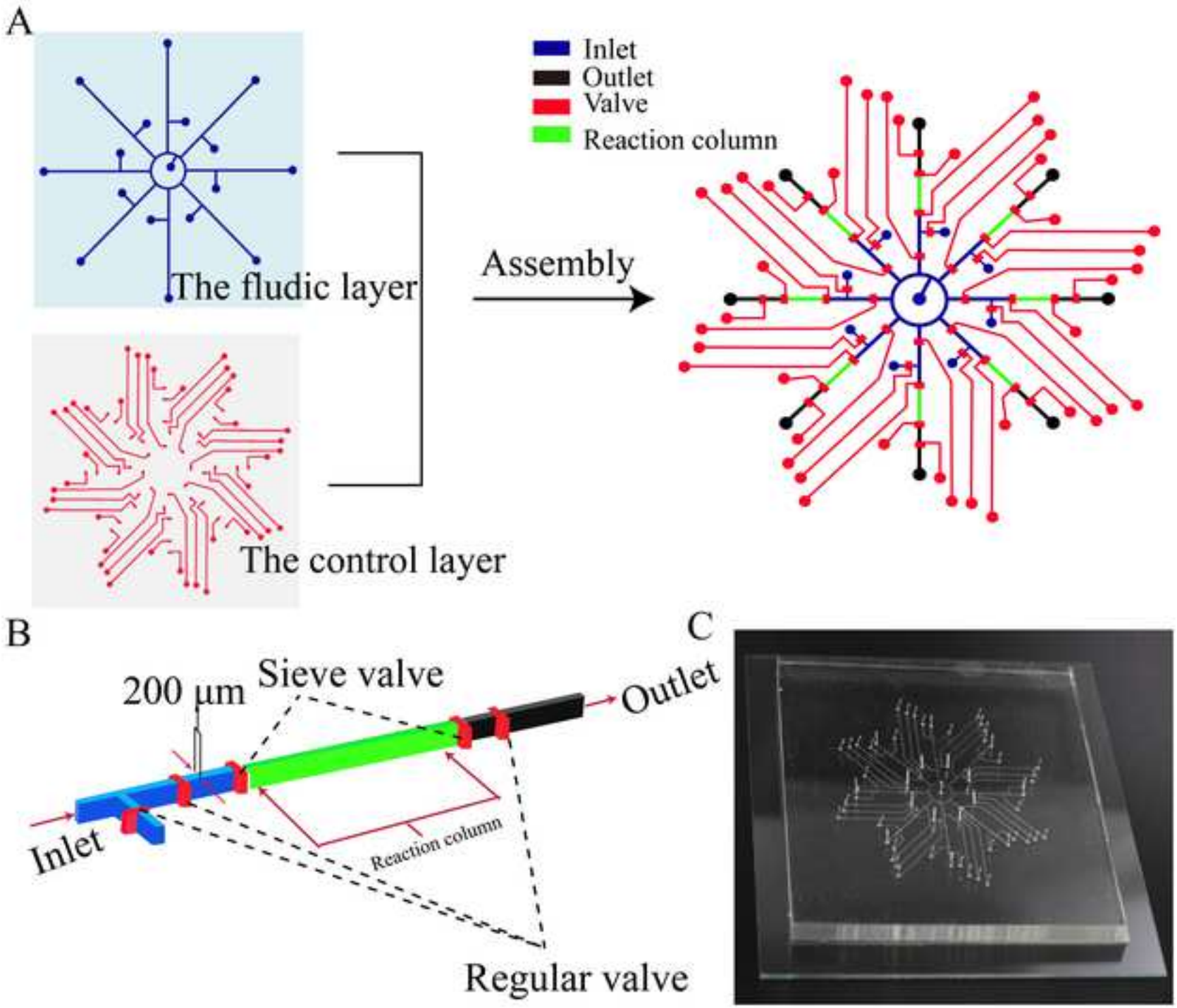

Figure 4

Click here to access/download;Figure;Figure 4.jpg

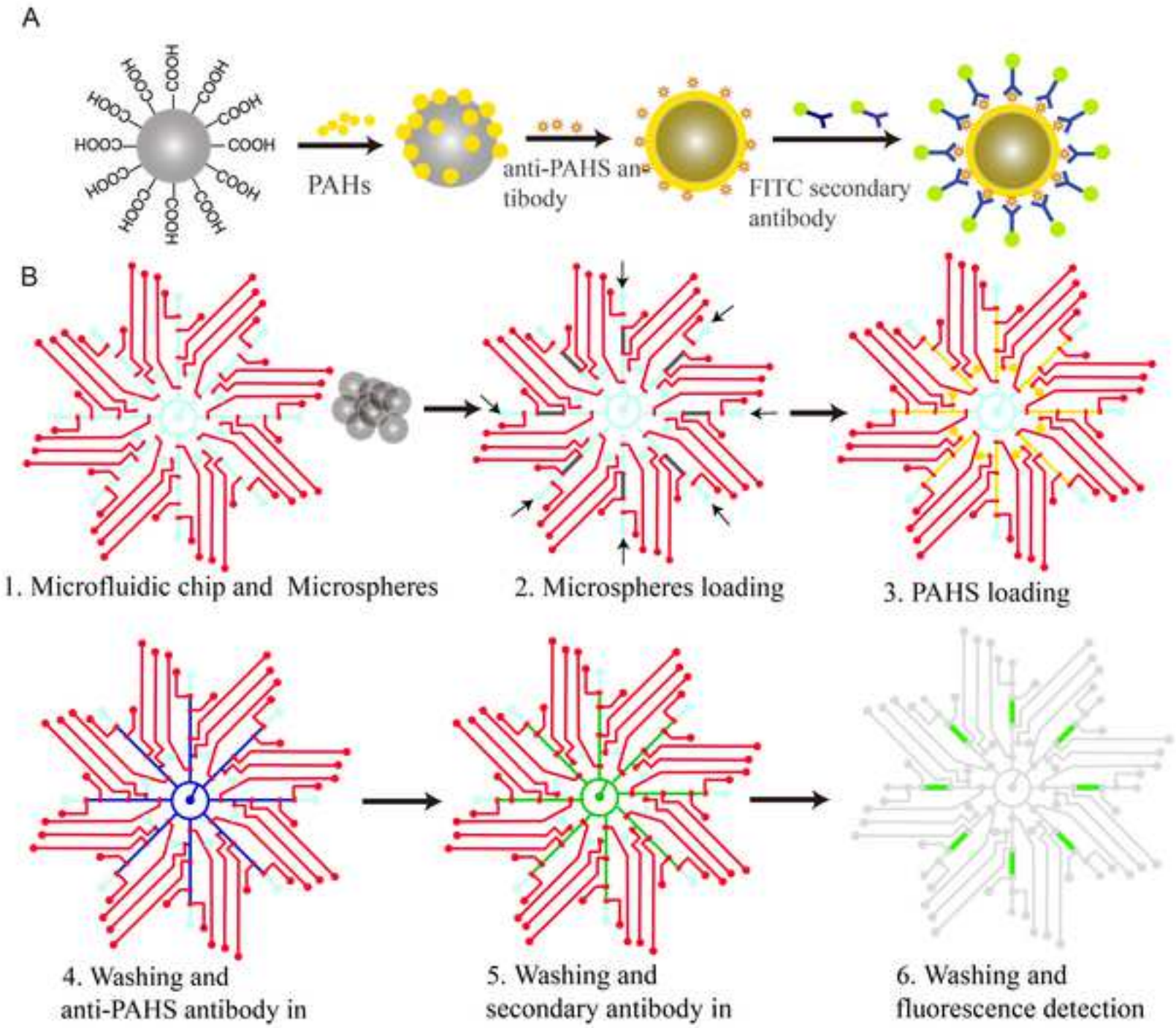

Figure 5

Click here to access/download;Figure;Figure 5.jpg

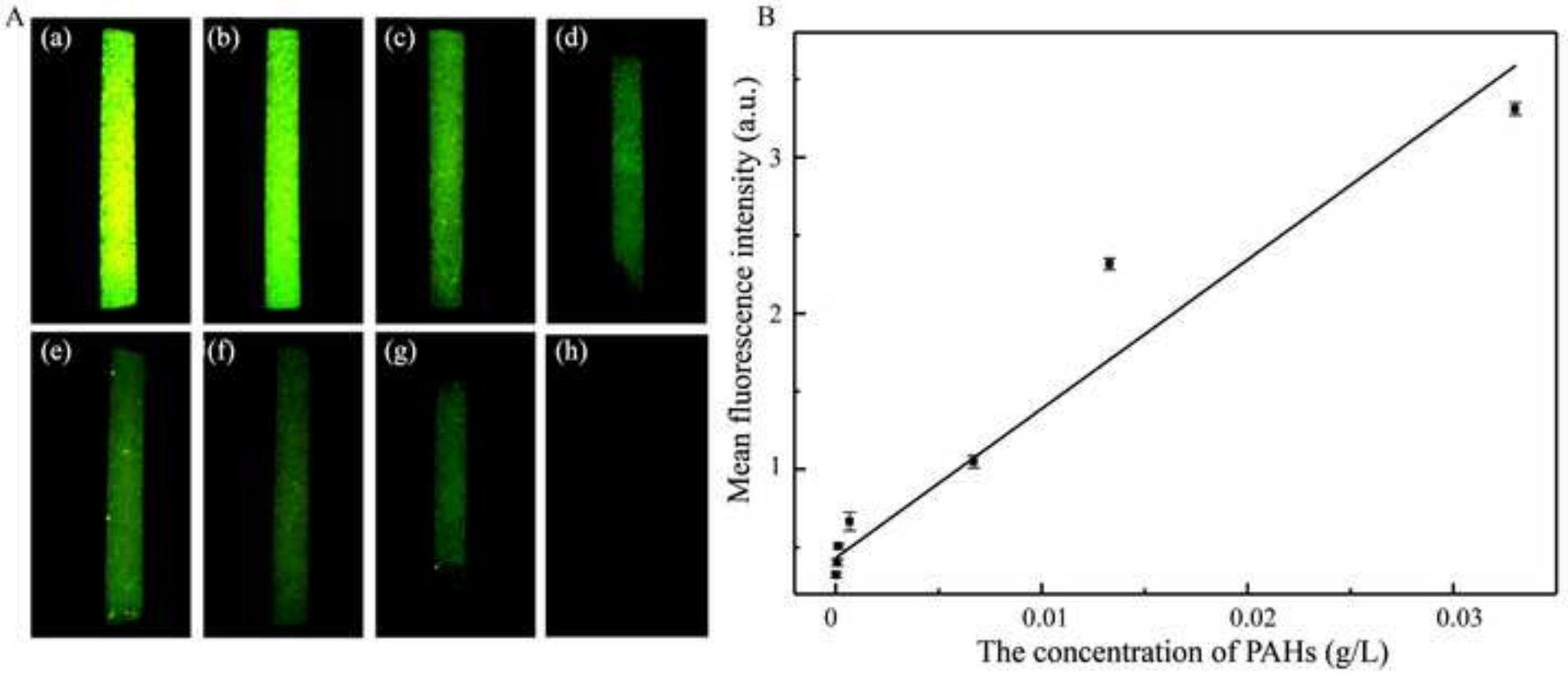

Figure 6

Click here to access/download;Figure;Figure 6.jpg

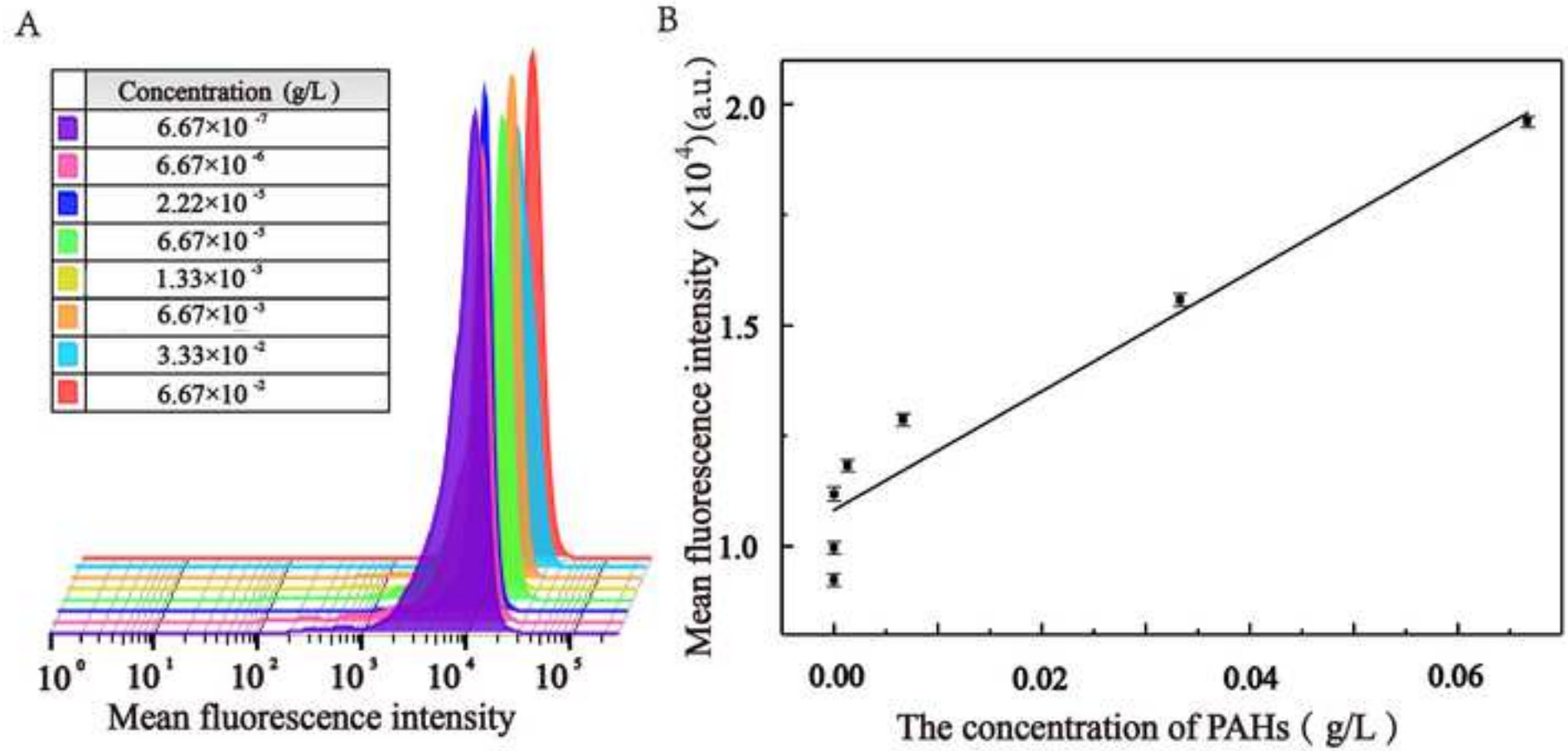

Figure 7

Click here to access/download;Figure;Figure 7.jpg

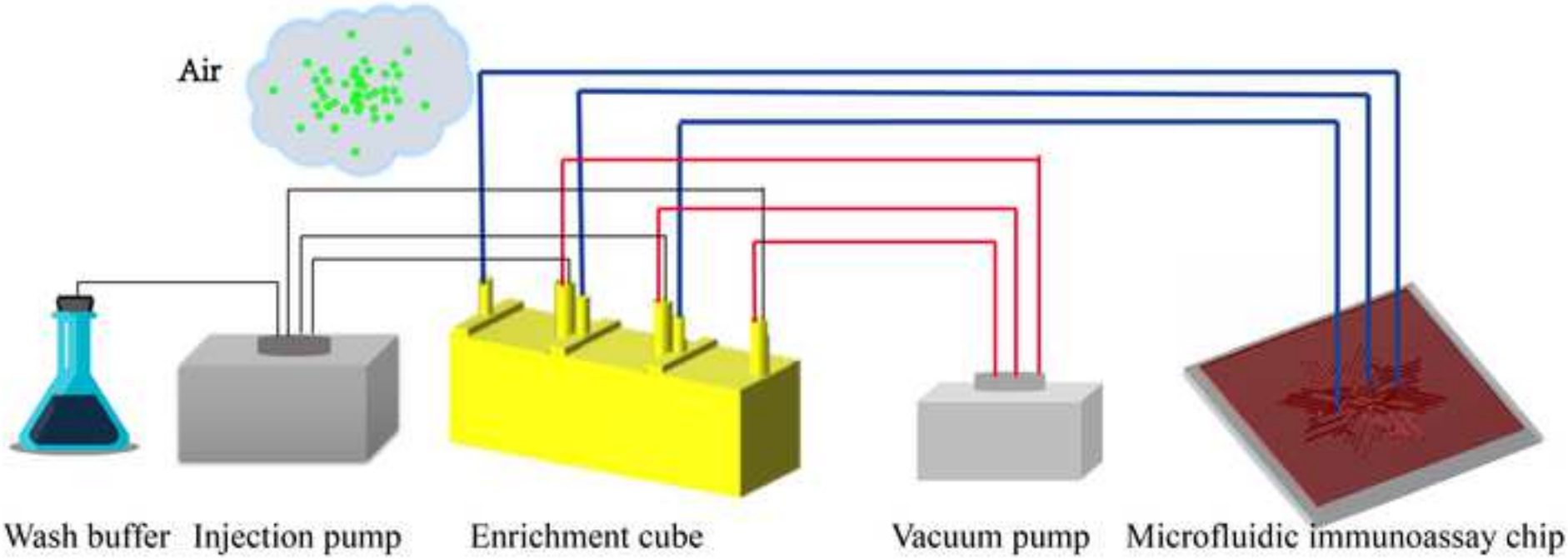

Figure 8

Click here to access/download;Figure;Figure 8.jpg

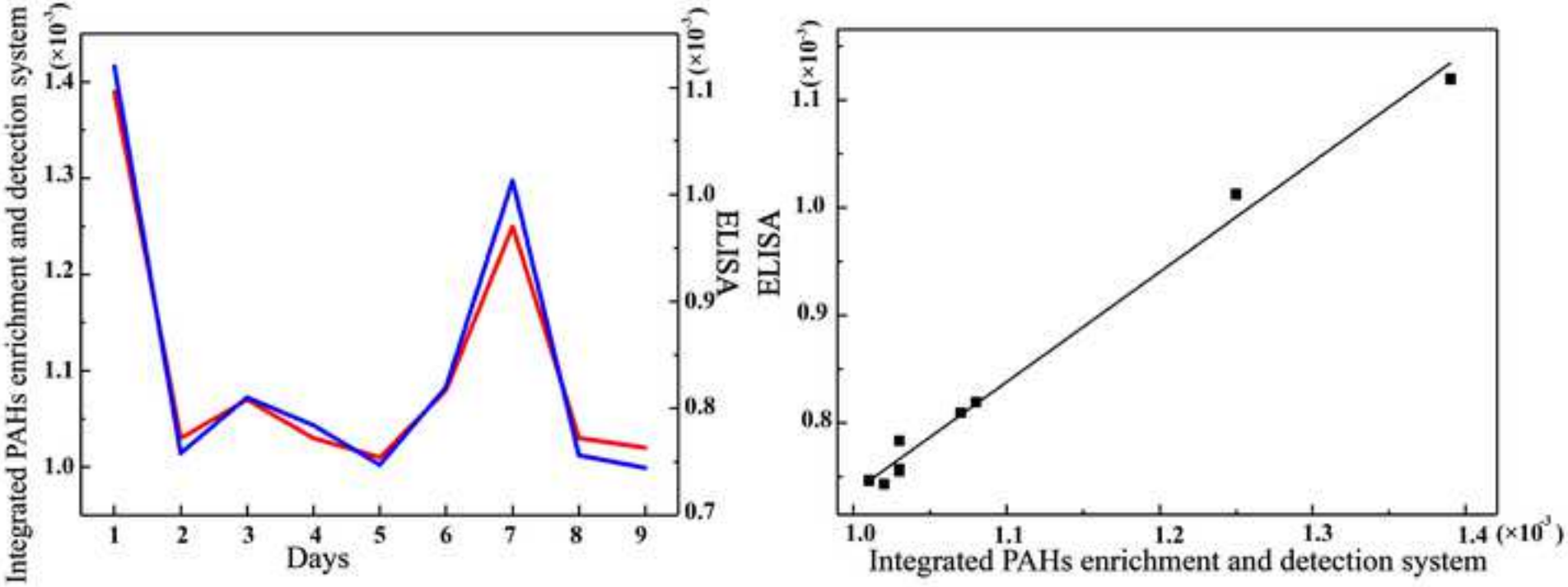

Declaration of interests

✓ The authors declare that they have no known competing financial interests or personal relationships that could have appeared to influence the work reported in this paper.

☐The authors declare the following financial interests/personal relationships which may be considered as potential competing interests:

Credit Author Statement

Lulu Zheng: Conceptualization, Methodology, Investigation, Writing - Original Draft. **Mantong Zhao:** Conceptualization, Methodology, Writing - Original Draft. **Bo Dai:** Methodology, Software, Investigation. **Zhiwei Xue:** Software, Investigation. **Yi Kang:** Software, Investigation. **Sixiu Liu:** Writing - Reviewing & Editing, Supervision. **Lianping Hou:** Supervision, Validation. **Songlin Zhuang:** Supervision, Validation. **Dawei Zhang:** Writing - Reviewing & Editing, Supervision.